JOURNAL OF SOLID STATE CHEMISTRY **128,** 176–180 (1997)
ARTICLE NO. SC967166

Modification of ZnO Thin Films by Ni, Cu, and Cd Doping

A. E. Jiménez-González

Laboratorio de Energía solar-IIM, Universidad Nacional Autónoma de México, Apartado Postal 34, 62580 Temixco, Morelos, Mexico

Received March 29, 1996; in revised form September 18, 1996; accepted September 24, 1996

With the propose of investigating the effect of transition elements in ZnO thin films prepared by the Successive Ion Layer Adsorption and Reaction (SILAR) technique, the deposition solutions were chemically impurified with Ni, Cu, and Cd, as elements of the Ib, IIb, and VIIIa groups. X-ray fluorescence (XRF) analyses confirm that the impurification with Ni and Cu in fact took place but the impurification with Cd did not, while the XRD analyses show that for *as prepared* and Ni-impurified annealed films, the crystallites are almost oriented along the *c* axis. The electrical properties of the ZnO films were also modified with the impurification. After annealing in air (450°C) the dark conductivity of the films was increased in the case of Ni and Cd impurification up to 1.80×10^{-3} and 1.86×10^{-2} $[\Omega\ \mathrm{cm}]^{-1}$, respectively, but it decreased drastically in the case of Cu to 5.51×10^{-7} $[\Omega\ \mathrm{cm}]^{-1}$, as referred to the dark conductivity (1.86×10^{-4} $[\Omega\ \mathrm{cm}]^{-1}$) of the pure ZnO sample. The measured activation energy for the electrical conductivity of the modified ZnO thin films is 55 meV for the Ni modification, indicating the existence of donor levels. On the other hand, the Cu modification increases the activation energy up to 132 meV, which is higher than the activation energy for pure ZnO thin films (98 meV). © 1997 Academic Press

1. INTRODUCTION

Pure and doped ZnO thin films have been the subject of much investigation in the past because the ZnO system has many important technological applications. Some of these are as luminescent materials (1), electroacoustic transducers (2), electrophotography (3), gas sensors (4), heterojunction solar cells (5), conductive transparent conductors (6), and heat mirrors (7). Pure ZnO thin films are not stable in air or in corrosive environments. Their electrical properties are significantly altered by adsorption of O_2, CO_2, CH groups, S compounds, and water. Therefore, single crystals and polycrystalline films of ZnO have been doped to enhance their properties with elements of the groups Ia, Li (8), and IIIb to VIIb, like Ga (9), ln (6, 10), N (1), Al (11, 12), Sn (13), P (14), etc. Doping was usually not done with transition elements of the groups Ib, IIb, and VIIIa. This is probably due to the incompatibility in the electron affinity or in the ionic radii of such elements with Zn.

With the intention to find new materials for the applications mentioned, we tried the impurification of ZnO thin films by the Successive Ion Layer Adsorption and Reaction (SILAR) technique with elements of the groups Ib, IIb, and VIIIb, like Ni, Cu, and Cd, respectively. The modifications brought about in the crystal structure and in the electrical properties, like electrical conductivity, photoconductivity, and activation energy, have been studied. The studies show significant modification of these properties through such doping.

2. EXPERIMENTAL

The ZnO thin films were prepared by the chemical deposition technique SILAR (Successive Ion Layer adsorption and Reaction), which was originally reported by Ristov *et al.* (15). The experimental setup and the details of the SILAR deposition technique used in the present work are reported elsewhere (16). The chemical solution was prepared in the following form: 15 ml of $NH_4(OH)$ was slowly added to 10 ml of 1 *M* $ZnSO_4$ solution and diluted in 250 ml water to form a tetraamminezinc (II), $[Zn(NH_3)_4]^{2+}$, complex. The impurification in each case was achieved by addition of $NiCl_2\cdot6H_2O$, $CuCl_2\cdot2H_2O$, or $CdCl_2\cdot2.5H_2O$ in the chemical solution 9 at.% of Ni, 13.7 at.% of Cu, or 12 at.% of Cd. The deposition process involved successive immersion of a glass substrate (Corning, Mexico; $75\times25\times1$ mm) in the solution (adsorption of the $[(NH_3)_4]^{2+}$ complex) and in hot water at 96°C (conversion of the complex to $Zn(OH)_2$ and ZnO). One cycle of the deposition in the present case gave a film thickness of approximately 25 Å and the deposition of each film was done with 30 immersion cycles (750 Å) (16). The impurified ZnO thin films were treated in air after the deposition for 2 h at 450°C.

The identification of the crystal structure was carried out with Cu$K\alpha$ radiation in a Siemens D-500 XRD-system. X-ray fluorescence measurements (XRF) were done in a Siemens SRS 303 spectrometer using a LiF single crystal oriented in the [110] direction. Photoresponse measurements were carried out in a computerized system using an HP 4140B picoammeter/DC voltage source. Pairs of silver electrodes were painted on the films for electrical contact at

0022-4596/97 $25.00

a distance of 5 mm and each were 5 mm long. An Oriel solar simulator using a xenon discharge lamp was used as the light source producing 900 Wm^{-2} of radiant intensity at the plane of the sample.

3. RESULTS AND DISCUSSION

3.1. XRD Analysis

Figure 1 shows the X-ray diffraction pattern of *as prepared* ZnO films impurified with (a) Ni, (b) Cu, and (c) Cd. All the three XRD patterns correspond to zincite structure (hexagonal ZnS, JCPDS 5-0664; $a = 3.249$ Å and $c = 5.205$ Å), but with different characteristic features. If we compare the spectra from Fig. 1 with the X-ray spectrum from ZnO powder (JCPDS 5-0664), then we find differences only in the relative peak intensities. In ZnO powder (not oriented) samples, the relative intensities (I/I_0) for the most dominant peaks are 71, 56, and 100% for the (100), (002), and (101) reflections, respectively. In the case of Ni impurification (Fig. 1a), the relative intensities are 5, 100, and 4.3% for the above-mentioned reflections. The crystallites are very strongly oriented along the *c* axis, [002] direction, perpendicular to the plane of the substrate. The impurification with Ni seems to occur through substitution of Zn cations by Ni ions, because there is no distortion of the crystal structure of ZnO. At the same time, the background of the pattern due to the glass substrate is very low. For the Cu and Cd impurification, the relative intensities are 50, 100, and 58% and 24, 100, and 66%, respectively, as shown in Fig. 1b and 1c. Thus, the *as prepared* films for the three cases of impurification have the crystallites preferentially oriented along the *c* axis. The XRD spectrum of pure ZnO film prepared by the SILAR technique (16) (not shown in Fig. 1) seems very similar to that represented in Fig. 1b.

Figure 2 shows the XRD pattern of the same films as in Fig. 1, but heated at 450°C in air for 2 h. We observe the same crystal structure, but with changes in the relative intensities among the peaks. In the case of Ni impurification, the relative intensities have changed to 45, 100, and 45% for the (100), (002), and (101) reflections. The peak intensities of the (100) and (101) reflections have increased, but the crystallites are still predominantly oriented in the [002] direction. Therefore, the impurification of ZnO with Ni promotes the grain orientation and maintains it even after the annealing. It has positive consequences on the electrical conductivity of ZnO, as will be seen later. For Cd and Cu impurification the relative intensities are 87, 92, and 100% and 91, 100, and 88%, respectively, indicating that for these cases a preferential orientation of the grains is gradually lost. The XRD spectrum of the pure *as prepared* ZnO thin film annealed in the same way (16) is very similar to the one corresponding to that given in Fig. 2b.

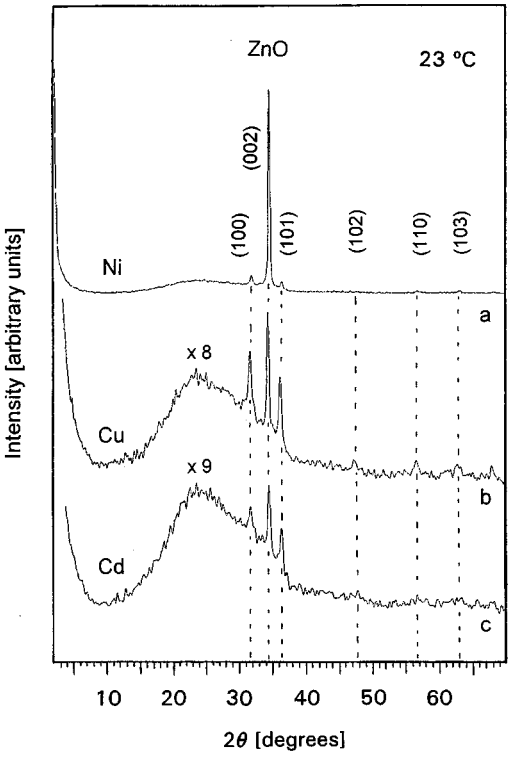

FIG. 1. X-ray diffraction patterns of *as prepared* ZnO thin films (thickness, 750 Å) impurified with (a) Ni, (b) Cu, and (c) Cd.

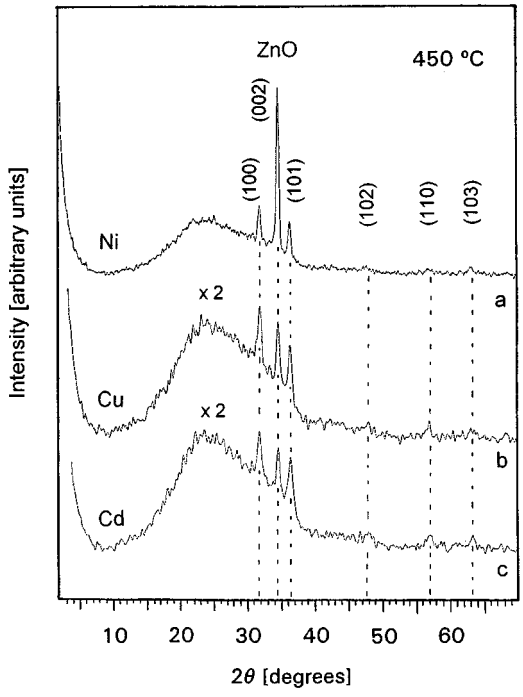

FIG. 2. X-ray diffraction pattern of ZnO thin films (thickness, 750 Å) treated in air at 450°C for 2 h and of these impurified with (a) Ni, (b) Cu, and (c) Cd.

3.2. XRF Analysis

Figure 3 shows the XRF spectra of ZnO thin films impurified with (a) Cu and (b) Ni. We observe the $K\alpha_1$ fluorescence signals for Cu at $2\theta = 65.6^\circ$ (Fig. 3a) and for Ni at $2\theta = 71.3^\circ$ (Fig. 3b). In the case of the Cd impurification, it was impossible to detect any trace of it by XRF in the deposited film. That means that the impurification with Ni and Cu in fact took place, but the impurification with Cd did not. The cadmium complex in the solution could act as a homogenizer (dispersive) agent. The lack of Cd incorporation is not due to incompatibility in the electronegativity: the relative electronegativity between the Cd and Zn cations is 0.92, 8% deviation. It is very probable that the incorporation did not take place due to the incompatibility between the ionic radii of Zn^{2+} (0.60 and 0.68 Å in coordination (IV) and (VI), respectively) and Cd^{2+} (0.78 and 0.95 Å in the same configurations, respectively) (17). Unlike in the case of Cd, the ionic radii of Ni^{2+} (0.55 and 0.63 Å), Cu^{+} (0.60 and 0.77 Å), and Cu^{2+} (0.57 and 0.73 Å) in the coordination (IV) and (VI), respectively, are not too different compared to the corresponding ionic radii of Zn^{2+}. We note that the concentration of the transition elements in the solution was intentionally chosen to be large (9 at.% Ni, 13.7 at.% Cu, and 12 at.% Cd, respectively) to ensure the detection of these elements in the films. It may be possible to try still lower concentrations.

3.3. Electrical Conductivity and Photoconductivity

Figure 4 shows the photoresponse curves of ZnO thin films impurified with (a) Cu, (d) Ni, and (e) Cd. For reference the photoresponse signal of the pure *as prepared* ZnO at 23°C (Fig. 4b) and treated at 450°C (Fig. 4c) are also shown. The dark current of the *as prepared* ZnO films is 1×10^{-10} A ($\sigma_{dark} = 5.6 \times 10^{-7}$ $[\Omega\,cm]^{-1}$) and its photocurrent is 1.1×10^{-4} A ($\sigma_{photo} = 0.8$ $[\Omega\,cm]^{-1}$). After annealing, the pure ZnO film presents a dark current of 2.7×10^{-8} A ($\sigma_{dark} = 1.862 \times 10^{-4}$ $[\Omega\,cm]^{-1}$) and a photocurrent of 1.8×10^{-4} A ($\sigma_{photo} = 1.0$ $[\Omega\,cm]^{-1}$). We observe in Fig. 4a that the impurification with Cu decreases drastically the dark and photocurrents of ZnO. The dark current achieves a value of 8×10^{-11} A ($\sigma_{dark} = 5.5 \times 10^{-7}$ $[\Omega\,cm]^{-1}$) and the photocurrent, a value of 1.5×10^{-9} A ($\sigma_{photo} = 5.5 \times 10^{-6}$ $[\Omega\,cm]^{-1}$).

Copper doped ZnO thin films have the lowest dark current probably because copper(II) takes electrons from the ZnO matrix to build Cu(I) to form Cu_2O or Cu_2O/CuO (not detected with XRD) and thus does not contribute to the electrical conductivity. Another explanation is based on the creation of deep donor levels, which would contribute to the low electrical conductivity only if thermally activated. This is supported by the activation energy of 132 meV observed in the sample as given in Section 3.4. We observe also from Figs. 4a, 4b, and 4c that copper also destroys the high photosensitivity of the ZnO films. Referred to the pure ZnO sample (Fig. 4c), we observe in Fig. 4d that the impurification with Ni enhances the dark current by one order

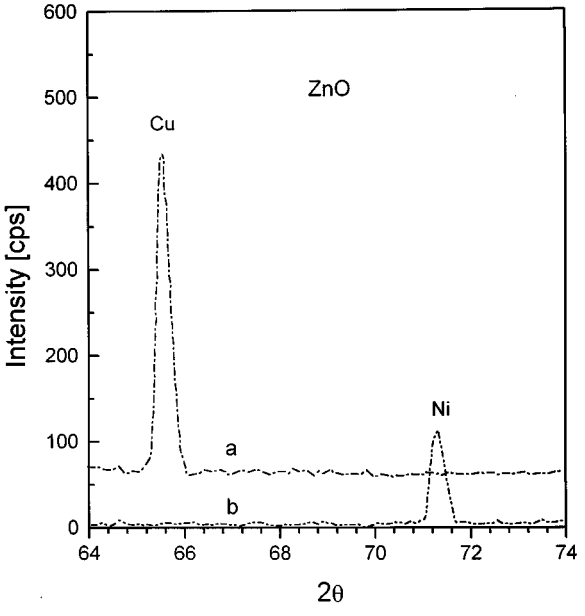

FIG. 3. X-ray fluorescence pattern of ZnO thin films treated in air for 2 h at 450°C and those impurified with (a) Cu and (b) Ni. The peaks correspond to Cu- and Ni$K\alpha_1$ radiation detected using LiF (110) planes.

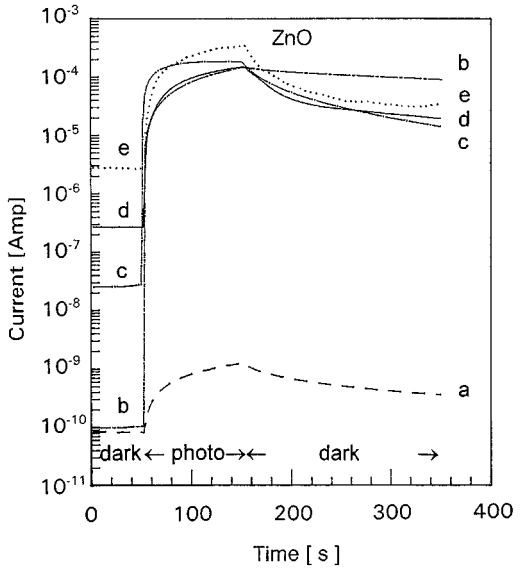

FIG. 4. Photoresponse measurements of annealed ZnO thin films impurified with (a) Cu, (d) Ni, and (e) Cd. The photoresponse curves of a pure *as prepared* ZnO thin film at (b) 23°C and treated at (c) 450°C are given for reference.

($\sigma_{dark} = 1.79 \times 10^{-3}$ $[\Omega\,cm]^{-1}$) probably due to the formation of bonds with Ni(II) and Ni(III) cations. The last case would contribute one free electron per cation and hence increase the electrical conductivity. The electrical properties (dark conductivity and photoconductivity) of the new system ZnO:Ni seems very similar to other systems like ZnO:Sn (14) and SnO:I (18).

Although the impurification with Cd does not take place, visually the films are more homogeneous at the surface than pure ZnO thin film. Therefore, the crystal homogeneity diminishes the electrical resistivity due to reduction in surface scattering processes, so that the dark current signal achieves a value of 2.8×10^{-6} A ($\sigma_{dark} = 1.86 \times 10^{-2}$ $[\Omega\,cm]^{-1}$). This is the maximum dark conductivity value among the films shown in Fig. 4. An explanation for this result may be based on the inhibition of oxygen incorporation in the intergrain region due to the Cd^{2+} present in the chemical solution. The reduction in oxygen incorporation would lead to a reduction in the depletion layer width and consequently enhancement of the effective carrier density in the grains (19). The photocurrent in ZnO "impurified" with Cd attains a value of 3×10^{-4} A ($\sigma_{photo} = 1.1$ $[\Omega\,cm]^{-1}$). The photocurrent decay in Figs. 4b–4e are very slow due to trapping centers introduced during the film preparation.

In general, ZnO doping with several cations of higher valence than zinc (Zn^{2+}), leading to increase in the electrical conductivity, have been reported by many researchers. Beginning with an intrinsic and undoped ZnO single crystal (4×10^{-3} $[\Omega\,cm]^{-1}$) (20), several conductivity values have been achieved after doping with metal elements of the groups IIIb to VIIb, like Ga (9), ln (6, 10), Al (11, 12), and Sn (13). For example, in the case of pellets, aluminum doped ZnO shows an electrical conductivity of 1 $[\Omega\,cm]^{-1}$ at 400°C (21), while gallium doped ZnO presents a very high dark conductivity of 300 $[\Omega\,cm]^{-1}$ (9). For thin films, gallium doped ZnO present one of the highest conductivity values achieved, 1.5×10^{3} $[\Omega\,cm]^{-1}$ (9), which is comparable with that of ZnO:Al with an electrical conductivity of 5.26×10^{3} $[\Omega\,cm]^{-1}$ (11). Both doped ZnO films were grown by the deposition technique rf-magnetron sputtering. Finally, regarding the electrical conductivity of ZnO doped with elements of the groups IIIb to VIIb let us assume that the electrical conductivity of the ZnO doped with transition elements can be improved in a great form by optimization of several experimental parameters like doping concentration, higher temperature treatment, and oxygen annealing.

Electrical conductivity changes due to a crystal reorientation have to be considered for *as prepared* and annealed samples. As shown in Fig. 1, all films have crystallites predominantly oriented along the *c* axis and at the same time they present a low dark current, as described in Fig. 1b for pure ZnO. After heating at 450°C some of the crystallites lose their preferred orientation along the *c* axis and this leads to an increase in the dark conductivity of pure, Ni- and Cd-impurified ZnO thin films. An explanation for this result may be the orientation loss and a diminishing grain size (20–30 Å) (22) of the crystallites, which contribute to the conductivity increase, due to an increase of the electron density in the conduction band. Another contribution to the dark current after the annealing is the formation of oxygen vacancies and cation interstitials, as already discussed for the case of pure ZnO (22). In the case of doping with Cu, these films gradually lose the preferred orientation without a dark current increase taking place. This means that the crystal reorientation does not contribute significantly to the dark current.

3.4. Activation Energy Determination

The activation energy E_{act} for the electrical conductivity in the case of *n*-type semiconductors is known as the energy difference between the conduction band and the donor levels, $E_C - E_D$. Major *et al.* (10) found that in ZnO thin films deposited by spray pyrolisis, the electrical conductivity of the films due to the free carrier concentration, *n*, in the conduction band is also dependent on the trap states located at the energy E_t below the conduction band, E_C, as

$$n = N_C \exp[-(E_C - E_t)/kT], \qquad [1]$$

where N_C is a function of the doping level, the density of states in the conduction band, the trap density, and the grain size, *k* is the Boltzmann constant, and *T* is the absolute temperature. If the temperature activated mobility is not the dominant process of the experiment (23), we can use Eq. [1] to calculate the activation energy of the ZnO thin films. Figure 5 shows the $\log(I)$ vs $1000/T$ $[K]^{-1}$ curves for (a) a pure ZnO film and for the same film but impurified with (b) Ni and (c) Cu. A temperature ramp of 7°C/min was used to heat the sample from 50°C ($1000/T$ $[K]^{-1} = 3.0$) to 250°C ($1000/T$ $[K]^{-1} = 1.9$) in vacuum (1×10^{-1} mbar). We find in this range of temperature linear behavior of the $\log(I)$ with the inverse of the temperature. The (negative) slope of the cases (a) and (b) are very small and they result from low activation energies. The activation energy, E_{act}, for the electrical conductivity of the films is 55 meV for the Ni modification. This corresponds to donor levels in the band gap of ZnO. These low activation energy values are the reason for the observed high dark current in Fig. 4d. Unlike the Ni case, the measured activation energy for the ZnO films impurified with Cu is 132 meV. The thermal energy at room temperature (26 meV) is not sufficient to induce the ionization of these deep levels. Another reason for the low electrical conductivity in this film at room temperature is that the Cu^{2+} (as deep donor center) traps electrons from the conduction band to be transformed in Cu^{+} (Fig. 4a). The activation energy for pure ZnO (Fig. 5a) is 98 meV. It is

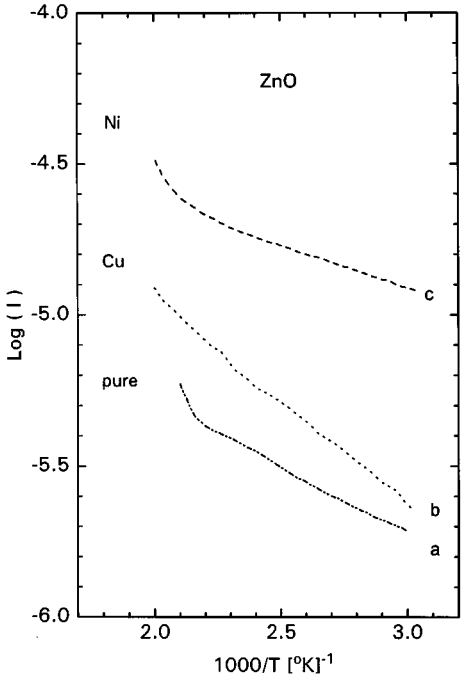

FIG. 5. Log (I) vs $1000/T$ $[K]^{-1}$ curves of (a) a pure ZnO thin film and of ZnO films impurified with (b) Cu and (c) Ni heated at 450°C in air, heating rate 7°C/min.

also a high value compared to the thermal energy at room temperature and hence leads to low dark conductivity.

4. CONCLUSIONS

We can conclude that the impurification of ZnO thin films prepared by the SILAR technique with Ni and Cu occurs successfully, as demonstrated with the XRF method, but the impurification with Cd does not. The Ni impurification increases the dark and photoconductivities of ZnO and favors the crystal growth with a preferred orientation of the crystallites in the *c* axis, which is retained even after the heat treatments in air at 450°C. Based on this result, Ni seems to be a good candidate for *n*-type doping of ZnO. In sharp contrast with this case, the impurification with Cu decreases the dark and photoconductivities and causes the randomization of the crystallites after the heat treatment. Cadmium acts as a homogenizer (dispersive) agent of the film during the crystal growth, which contributes to a reduction in surface scattering of charge carrier and an increase in the dark and photoconductivities. We found that ZnO thin films impurified with Ni are photoconductive, while Cu almost destroys the dark and photoconductivities. Optically, the ZnO thin films have 90% optical transmittance in the VIS and IR regions. ZnO films impurified with Ni assume a light blue tone, while those impurified with Cu assume a light brown color. In this way their optical transmittance changes slightly in the visible region. In the case of Cd, there is no notable coloration of the films. Each of the impurified ZnO thin films is very stable in air atmosphere, vacuum, and oxygen and under thermal treatments.

ACKNOWLEDGMENTS

The author is grateful to Dr. P. K. Nair for the revision of this manuscript, to Leticia Baños from III-UNAM for the XRD spectra, and to CONACYT for the financial support.

REFERENCES

1. H. C. Pan and B. W. Wessels, *Mater. Res. Soc. Symp. Proc.* **152,** 215 (1989).
2. H. W. Lehman and R. Widmer, *J. Appl. Phys.* **44,** 3868 (1973).
3. R. M. Schaeffert, "Electrophotography," p. 320. Focal Press, London, 1980.
4. L. M. Zav'yalova, E. E. Gutman, and Y. A. Myasnikov, *Zh. Fiz. Khim.* **53,** 2125 (1979).
5. B. M. Basol, V. K. Kapur, A. Halani, and C. Leidholm, "Annual Report, Photovoltaic Subcontract Program FY 1991" (K. A. Summers, Ed.), p. 7. NREL, Golden, CO, 1993.
6. K. L. Chopra, S. Major, and D. K. Pandya, *Thin Solid Films* **102,** 1 (1983).
7. Z. C. Jin and C. G. Granqvist, *Proc. SPIE* **21,** 823 (1987).
8. A. N. Gergobiani, T. V. Butkhuzi, O. V. Aleksandrov, and T. G. Khulordava, *Sov. Phys. Lebedov Institut Rep.* **9,** 53 (1984).
9. R. Wang and A. W. Sleigth, *Chem. Mater.* **8,** 433 (1996).
10. S. Major, A. Banerjee, and K. L. Chopra, *J. Mater. Res.* **1,** 300 (1986).
11. T. Minami, H. Nanto, and S. Takata, *Jpn. J. Appl. Phys. Lett.* **23,** 280 (1984).
12. K. Tominaya, M. Kataok, T. Uedo, M. Chong, Y. Shintani, and Y. Mori, *Thin Solid Films* **253,** 9 (1994).
13. M. Ristov, G. J. Shinadinovski, Y. Grozdanov, and M. Miterski, *Thin Solid Films* **149,** 9 (1987).
14. A. Kobayashi, O. F. Sankey, and J. D. Dow, *Phys. Rev B* **28,** 946 (1983).
15. M. Ristov, G. J. Shinadinovski, and Y. Grozdanov, *Thin Solid Films* **123,** 63 (1985).
16. A. E. Jiménez-Gonzailez and P. K. Nair, *Semicond. Sci. Technol.* **10,** 1277 (1995).
17. R. D. Shanon, *Acta Crystallogr. A* **32,** 751 (1976).
18. K. L. Chopra and S. R. Das, "Thin Film Solar Cells," p. 328. Plenum Press, New York, London, 1983.
19. J. W. Orton, B. J. Goldsmith, J. A. Chapman, and M. J. Powell, *J. Appl. Phys.* **53,** 1602 (1982).
20. G. Heiland, *Z. Phys.* **148,** 15 (1957).
21. K. Haufle and A. L. Vierk, *Z. Phys. Chem.* (*Frankfurt*) **196,** 160 (1950).
22. A. E. Jimenez-Gonzalez and R. Suarez-Parra, *J. Cryst. Growth* **167,** 649 (1996).
23. J. W. Orton and M. J. Powell, *Rep. Prog. Phys.* **43,** 1263 (1980).